Superlattices and Microstructures 46 (2009) 483–489

Contents lists available at ScienceDirect

Superlattices and Microstructures

journal homepage: www.elsevier.com/locate/superlattices

Preparation and characterization of the transparent SiO_2–Ag/PVP nanocomposite mirror film for the infrared region by sol–gel method

M.S. Sadjadi [a,*], N. Farhadyar [a], K. Zare [a,b]

[a] Department of Chemistry, Sciences and Research Branch, Islamic Azad University, Tehran, Iran
[b] Department of Chemistry, Shahid Beheshti University, Tehran, Iran

ARTICLE INFO

Article history:
Received 13 January 2009
Received in revised form
27 May 2009
Accepted 2 June 2009
Available online 17 July 2009

Keywords:
Transparent mirror coating
SiO_2–Ag/PVP nanocomposite
Dip coating technique
Silica modified PVP
Sol–gel method

ABSTRACT

Transparent mirror coated, SiO_2–Ag/PVP nanocomposites were prepared on the Pyrex glass slides by dip-coating technique. Embedding of the silver (Ag) nanoparticles on silica modified polyvinyl pyrrolidone (PVP) was performed by the sol–gel method. As prepared transparent mirror coated SiO_2–Ag/PVP nanocomposite films were finally characterized for surface morphology, chemistry, and nano size dimensions using various advanced analytical techniques including, UV visible, Fourier transform, infrared spectroscopy (FT-IR), X-ray powder diffraction (XRD), scanning electron microscopy (SEM), dispersive x-ray analaysis (EDAX) and transmission electron microscopy (TEM) analysis. It was found that all the prepared samples were almost uniform particles of Ag nanospheres of 7–8 nm diameters arranged as double paralleled nanowires with an average length of 200–450 nm and diameters of around 20–25 nm.

1. Introduction

In recent years, more and more researchers devote themselves studying composite nanomaterials. Since, the combination of different components in the nanosize range can yield new materials that may combine the advantages of each component and nanomaterials [1–3]. Among these composites, many recent efforts have been focused on the incorporation of inorganic nanoparticles and polymer materials. These efforts can offer opportunities to explore their novel collective mechanical, thermal, optical, magnetic and electronic properties [4–8]. Various methods such as synergic, grafting,

* Corresponding author. Tel.: +98 2122285032.
E-mail address: msadjad@gmail.com (M.S. Sadjadi).

0749-6036/$ – see front matter © 2009 Elsevier Ltd. All rights reserved.
doi:10.1016/j.spmi.2009.06.004

polymerization, sol–gel reaction and amphiphilic self-assembly have been applied to prepare the composite microsphere materials with required properties and structures [9–13].

In this paper, we report the synthesis of mirror coated SiO_2–Ag/PVP nanocomposite film on the Pyrex glass slides by dip-coating techniques. The embedding of silver (Ag) nanoparticles on silica modified (PVP) was performed by the sol-gel method by adding PVP to a partially hydrolyzed TEOS and silver nitrate ($AgNO_3$) solution.

2. Experiments

$AgNO_3$ was purchased from Fluka. PVP, $Mw = 400\,000$, TEOS and ethanol were supplied by Merck Co. (China). All chemical reagents were analytical grade and used without further purification.

Synthesis of Ag-SiO_2/PVP nanocomposite was carried out by the sol-gel method is given by the following steps:

- The hybrid sol was prepared by placing TEOS in a beaker with 0.01 M HCl (pH = 1). The molar ratio of H_2O/TEOS was 2/1 at room temperature. The resultant two-phase solution was vigorously stirred at a rate of 150 rpm for 3 h.
- Appropriate amounts of PVP and $AgNO_3$ were dissolved in ethanol/water (60/40, wt/wt) solution. The concentration of PVP was 8 wt%, and the weight of $AgNO_3$ was calculated on the basis of the weight of PVP. The mole ratio of PVP and $AgNO_3$ was 10/1. Upon swift injection of the mixture obtained in this step into the reaction system prepared in step I and stirring the mixture rapidly, a transparent hybrid sol mixture of SiO_2–Ag/PVP was formed.
- The Soda Lime Glass slides, used as substrates for the sol-gel coatings were initially rinsed with DI H_2O and etched with 0.01 M NaOH solution. The substrates were rinsed with DI H_2O again and then immersed in 0.01 M HCl solution to remove excess of NaOH solution from the substrate's surface. Each substrate was then cleaned with hexane and methanol to remove all the dirt, grease and was then air dried.
- Coating and cured films with different thicknesses were prepared, as a function of time and viscosity. Coating experiments were carried out by a dip coating technique on the thin soda lime glass slides used as substrates [9]. Cleaned glass slides were immersed into the hybrid sol mixture prepared in the above cited steps for 1 min and drawn up vertically. The coated films were air dried onto the substrate and placed in a furnace to cure at the temperatures of 165 °C for 150 min.

The UV–Visible spectrum in absorbance mode was recorded on a UV–Visible Hitachi spectrophotometer model U-2101 PC. The solution form of the sample was prepared by suspending a small amount of powder in ethanol. The FTIR characterization of pure PVP, sol of SiO_2–Ag/PVP before curing and finally SiO_2–Ag/PVP nanocomposite coatings was carried out by using a Perkin Elmer IF 66/5 spectrophotometer. The spectra were obtained in KBr pellets. The Powder X-ray diffraction (XRD) pattern was recorded on a Seisert Argon 3003 PTC using nickel-filtered XD-3a Cu Kα radiations ($\lambda = 1.5418$ Å). A Philips EM208 and microscope operated at 100 kV transmission electron microscope (TEM) was used to observe the morphology and size distribution of Ag nanoparticles. The samples were prepared by carbon-coated copper grids. Scanning electron microscopy (SEM) images of the prepared silver nanocomposites were obtained using a Philips electron microscope equipped with a Dispersive analysis of X-RAY (EDAX). The samples were rinsed with distilled water, dried and coated with a thin layer of gold by evaporation in a vacuum to form conducting film.

3. Results and discussion

3.1. UV–Visible analysis

Fig. 1 represents the UV–Visible absorption of as prepared Ag/PVP and SiO_2–Ag/PVP. This figure shows a broad absorption characteristic band at $\lambda_{Max} = 410$ nm due to the oscillation of conduction band electrons of Ag, known as the surface plasmon resonance [14–19]. The position of the plasmon absorption bands depends on particle size, aspect ratio and diameter of embedded nanoparticles [20]. The broad nature of the absorption bond in this case is indicative of the presence of both sphere and embedded nanoparticles in SiO_2 modified PVP.

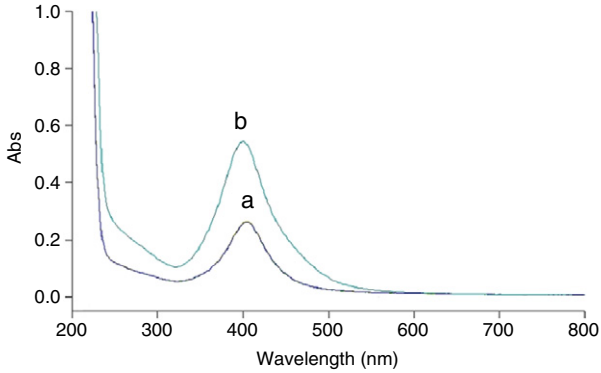

Fig. 1. The UV–Visible absorption of as prepared (a) Ag/PVP, (b) SiO_2–Ag/PVP.

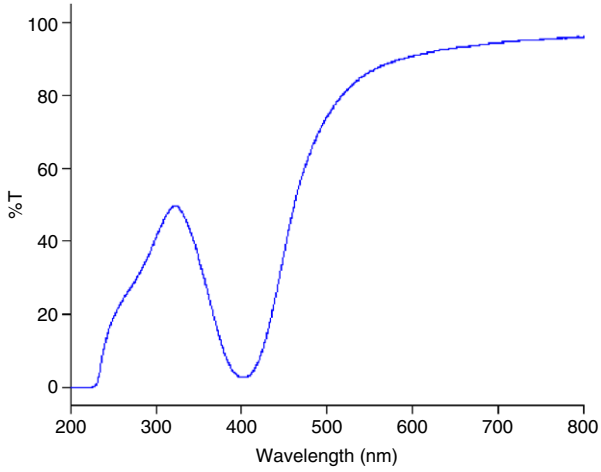

Fig. 2. Transmittance of as prepared SiO_2–Ag/PVP nanocomposite coated films.

3.2. Transparency analysis

Fig. 2 represents transmittance of as prepared SiO_2–Ag/PVP nanocomposite coating film on a glass slide. This Figure shows the Ag nanoparticle size dependent transparency of 96% in the infrared region.

3.3. FTIR analysis

Fig. 3(a)–(c) represent FTIR spectra of PVP and SiO_2–Ag/PVP nanocomposite films before and after curing. The figure shows that the peak of CO (at 1659) was weakened after curing and changed to 1655, but the peaks of C–N at (1017 and 1074) [21,22], and the strong bond frequency of Si–O bond at 1043 of non cured SiO_2–Ag/PVP sol (appeared upon addition of the silica solution) were strengthened and red shifted to 1074 and 1125 in the nanocomposite film after curing. These changes of the spectrum indicated that Ag nanoparticles were embedded in the SiO_2–Ag/PVP nanocomposite by coordination through the O atoms of PVP and SiO_2.

Though the pyrrolidyl has a steric effect on the coordination between N and Ag, the electronegativity of N was lower than that of O. Therefore, the electron donating capability of N is higher than that of O and N can be coordinated with silver ions or particles. So, for the particles with a shorter diameter, the steric effect is not the main factor that influenced the reaction between PVP

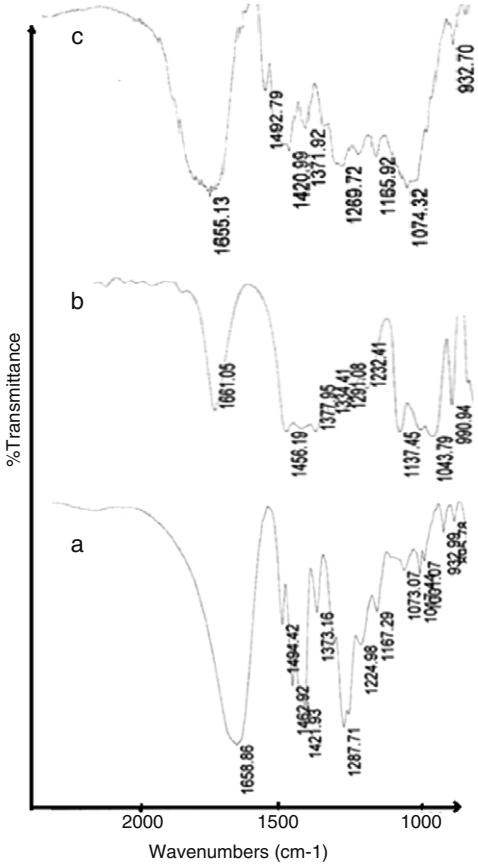

Fig. 3. FTIR Spectra of: (a) PVP, (b) SiO_2–Ag/PVP films before curing and (c) SiO_2–Ag/PVP coated films after curing.

and silver. This can be proved by IR spectrum of the sols before curing, in which the peak of CO (at 1659) was strengthened and shifted to 1661 (Fig. 3(b)). As a result the coordination between PVP and silver in the sol before curing can be considered not on O, but on N. When the particles size grew upon curing of the sol, the steric effect was important in the reaction between silver and PVP. In this case, steric effect will prevent the coordination between N and silver, and O will be coordinated with the silver particles. This can be seen and proved by the IR spectrum results for the samples after curing (as shown in Fig. 3(c)). In this spectrum, beside of the Si-O frequency strengthening (at 1043 of the non cured SiO_2–Ag/PVP sol), the peak of CO weakened and changed from 1659 to 1655. So, when the particles grew up, steric effect comes to be important in the reaction between silver and PVP, and O of PVP will be coordinated with the embedded silver nanoparticles in SiO_2–Ag/PVP composite.

3.4. XRD diffraction

A typical XRD pattern of as prepared SiO_2–Ag/PVP nanocomposite shows the presence of the diffraction peaks corresponding to the (111), (200), (220), (311) planes. All diffraction peaks in this XRD pattern (Fig. 4) can be well indexed as face-centered cubic silver with peak positions, indicating that the face-centered cubic (fcc) structure of the Ag is preserved in this nanoparticles embedded form (JCPDS, File No. 4-0783) [23]. These results indicate a polycrystalline structure for silver nanoparticles embedded in SiO_2–Ag/PVP with an intense (111) preferred orientation. Secondary peaks at (200) and (220), corresponding to the high angle XRD pattern ($2\theta = 30$–60), support the presence of the

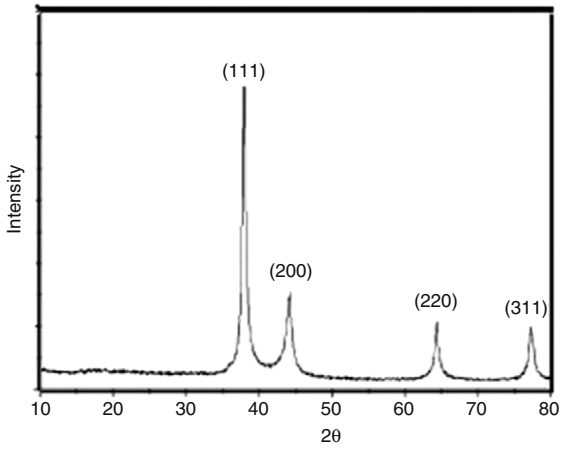

Fig. 4. XRD pattern of SiO_2–Ag/PVP nanocomposite indicating the face-centered cubic structure.

Table 1
EDAX ZAF Quantification of the percentage ratio of Ag, Si and oxygen in the prepared SiO_2–Ag/PVP nanocomposites mirror films.

Elements	Weight (%)	Atomic (%)
O	35.65	68
Si	39.77	24.82
Ag	24.58	7.18
	100	

face-centered cubic structure in the prepared SiO_2–Ag/PVP nanocomposite. The peaks appearing at ($2\theta = 38.4$) and ($2\theta = 44.6$) may be corresponded to the (111) and (200) planes of the silver lattice respectively.

The dimensions of the crystallite which the Ag nanospheres are embedded in silica modified PVP can be estimated from the Scherrer formula [24]. This equation is applicable to samples where lattice strain is absent. The Ag nanosphere in the present case may posses some strains, which could be a factor contributing to the width of the peaks, thereby affecting estimates of the crystallite size of the nanosphere [25]. The grain size of the silver nansphere estimated from the XRD peak width (and using Scherrer,s formula), was approximated to be 8.4 nm. The result that is approximately comparable with TEM results.

3.5. SEM Micrographs and dispersive x-ray analaysis (EDAX)

The SEM image of as prepared SiO_2–Ag/PVP nanocomposite is shown in Fig. 5. The morphology of the resulting surfaces, indicate that the composite coating structure can be considered as a mechanical mixture of homogenous polymer nanoparticles.

The X-RAY dispersive analysis (EDAX) of the samples shown in Fig. 6 and Table 1 give the percentage ratio of Ag nanoparticles, Si and oxygen in the SiO_2–Ag/PVP nanocomposite.

3.6. TEM Micrographs

TEM images of the SiO_2–Ag/PVP nanocomposites prepared by the controlled-concentration and curing temperature shown in Fig. 7(a),(b), illustrate individual Ag nanoparticles of 7–8 nm diameters as well as Ag nanospheres which are embedded on silica mediated PVP. Fig. 7(b) exhibits side section of the Ag nanosphere crystallite assembled in a bunch of peals on the surface of silica matrix with the average length of 200–450 nm and diameters of around 20–25 nm.

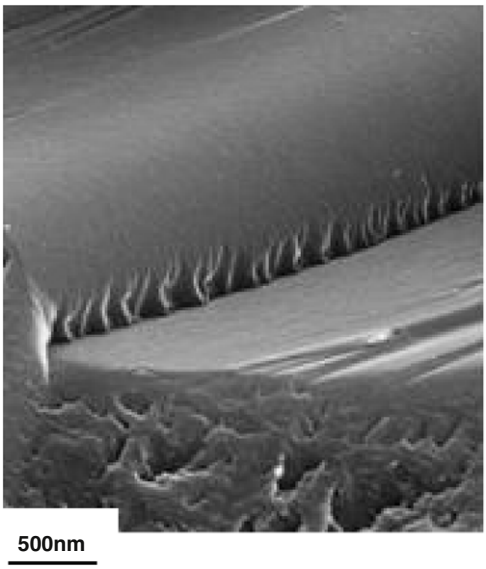

Fig. 5. SEM image of as prepared SiO_2–Ag/PVP nanocomposites illustrating homogenous mechanical mixture of the polymer of nanoparticles.

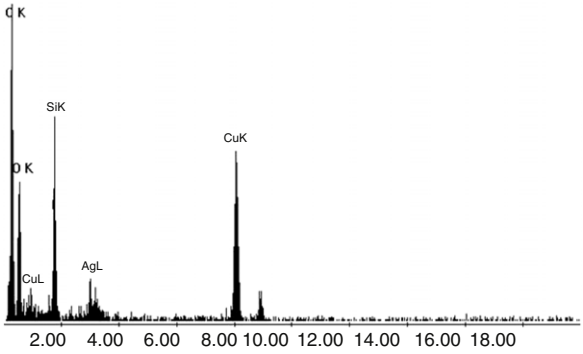

Fig. 6. EDAX analysis of as prepared SiO_2–Ag/PVP nanocomposite indicating the percentage ratio of Si, O and Ag nanoparticles.

4. Conclusion

We concluded that silica modified PVP is a remarkably powerful capping agent for the preparation of a 1D arrangement of Ag nanoparticles and prepared inorganic/organic nanocomposite can now be developed towards optical and medicinal based applications. The broad nature of the UV–Visible absorption band at $\lambda_{Max} = 410$ nm due to the oscillation of conduction band electrons of Ag indicated the presence of both embedded sphere and assembled nanospheres in SiO_2 modified PVP. Transparency dependent on the Ag nanoparticle size was about 96% in the infra-red region. The FTIR results indicated that the steric effect in the reaction between silver and PVP will be important when the particles size grow up upon curing of the sol and the main reaction between silver nanoparticles embedded in silica modified PVP may occur between O atoms of silica modified PVP and Ag nanoparticles. The XRD data confirmed that the Ag nanoparticles are crystalline with fcc structures having a preferred crystallographic orientation along the (220) direction. The grain size of the silver nanospheres estimated from the XRD peak width (and using Scherrer's formula), was about 8.4 nm. TEM observations from the side section of the prepared sample illustrated individual Ag nanosphere

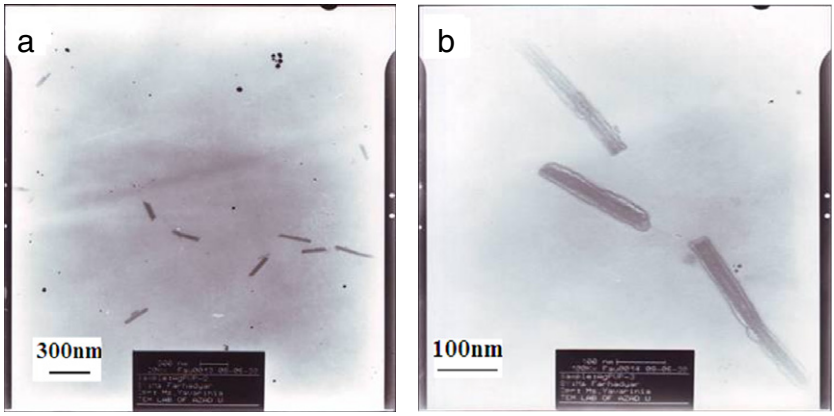

Fig. 7. TEM image of (a) Individual Ag nanospheres embedded on silica modified PVP, (b) side section of the Ag nanospheres crystallite assembled as a bunch of peals on the silica matrix surfaces.

crystallite of 7–8 nm diameters embedded as a bunch of peals on the surface of silica modified PVP with average length of 200–450 nm and diameters of around 20–25 nm.

Acknowledgements

The authors express their thanks to the Vice presidency of Science and Research Branch, Islamic Azad University and Iranian Nanotechnology Initiative for their encouragement, permission and financial support.

References

[1] A. Slistan-Grijalva, R. Herrera-Urbina, J.F. Rivas-Silva, M.A valos Borja, F.F. Castillo'n-Barraza, A. Posada-Amarillas, Physica E 27 (2005) 104.
[2] P.K. Khanna, N. Singh, S. Charan, V.V.V.S. Subbarao, R. Gokhale, U.P. Mulik, Mater. Chem. Phys. 93 (1) (2005) 117.
[3] G. Carotenuto, Appl. Organomet. Chem. 15 (5) (2001) 344.
[4] J.L. Elechiguerra, J.L. Burt, J.R. Morones, A. Camacho-Bragado, X. Gao, H.H. Lara, M.J. Yacaman, J. Nanobiotechnol. 3 (6) (2005).
[5] E.I. Suvorova, V.V. Klechkovskaya, V.V. Kopeikin, Ph.A. Buffat, J. Cryst. Growth 275 (1/2) (2005) e2351.
[6] I. Sondi, B. Salopek-Sondi, J. Colloid Interface Sci. 275 (2004) 177.
[7] M. Zheng, M. Gu, Y. Jin, G. Jin, Mater. Res. Bull. 36 (5/6) (2001) 853.
[8] G. Carotenuto, G.P. Pepe, L. Nicolais, Eur. Phys. J. B 16 (1) (2000) 11.
[9] F. Bonet, S. Grugeon, R. Herrera Urbina, K. Tekaia-Elhsissen, J.-M. Tarascon, Solid State Sci. 4 (5) (2002) 665.
[10] Y. Sun, Y. Xia, Science 298 (2002) 2176–2179.
[11] Y. Sun, B. Gates, B. Mayers, Y. Xia, Nano Lett. 2 (2002) 165.
[12] A. Slistan-Grijalva, R. Herrera-Urbina, J.F. Rivas-Silva, M.A valos Borja, F.F. Castillo'n-Barraza, A. Posada-Amarillas, Physica E 25 (2005) 438.
[13] B. Wiley, T. Herricks, Y. Sun, Y. Xia, Nano Lett. 4 (9) (2004) 1733.
[14] M.A.S. Sadjadi, Babak Sadeghi, M. Meskinfam a,b, K. Zare a,b, J. Azizian, Physica E 40 (2008) 3183–3186.
[15] T. Itakura, K. Torigoe, K. Esumi, Langmuir 11 (1995) 4129.
[16] C.A. Foss, G.L. Hornyak, J.A. Stockert, C.R. Martin, J. Phys. Chem. 98 (1994) 2963.
[17] S. Link, M.B. Mohamed, M.A. El-Sayed, J. Phys. Chem. B 103 (1999) 3073.
[18] N.R. Jana, L. Gearheart, C.J. Murphy, J. Phys. Chem. B 105 (2001) 4065.
[19] V.M. Cepak, C.R. Martin, J. Phys. Chem. B 102 (1998) 9985.
[20] P.K. Khanna, N. Singh, S. Charan, V.V.V.S. Subbarao, R. Gokhale, U.P. Mulik, Mater. Chem. Phys. 93 (2005) 117.
[21] H. Wang, et al., Mater. Chem. Phys. 94 (2005) 449–453.
[22] V.A. Breshtein, V.A. Ryzhov, Adv. polym. Sci. 43 (1994) 114.
[23] JCPDS Silver file 04-0783.
[24] B.D. Cullity, Elements of X-ray Diffraction, second ed., Addison-Wesley, Reading, MA, 1978.
[25] Y. Wang, Y. Li, S. Yang, G. Zhang, D. An, C. Wang, Q. Yang, Y. Wei, Nanotechnol. 17 (13) (2006) 3304–3307.